

Zinc sulfide nanoparticles: a mechanism of formation in aqueous solutions and optical properties

T. N. Shcherba, K. V. Lupandina, M. P. Zhilenko,* G. P. Muravieva, H. V. Ehrlich, and G. V. Lisichkin

Chemical Department, M. V. Lomonosov Moscow State University,
1/3 Leninskie Gory, 119991 Moscow, Russian Federation.
Fax: +7 (495) 932 8846. E-mail: Zhilenko@petrol.chem.msu.ru

The formation of sols and precipitates of zinc sulfide as a result of the exchange reaction in an aqueous solution was studied. The precipitates consist of aggregates of primary particles about 3 nm in size. The primary ZnS particle size in aqueous sols increases with an increase in the concentration of zinc sulfate and sodium sulfide, with the accumulation of the final reaction product, and with temperature. This effect does not exceed an 1.5-fold increase. At the first step, the particles with a considerable fraction of the amorphous phase are formed and undergo intragrain crystallization. The photoluminescence properties of aqueous sols of zinc sulfide were studied. They are caused by defects in the ZnS lattice and by the presence of the lattice oxygen.

Key words: nanoparticles, zinc sulfide, size effects, lattice defects, luminescence.

Luminescent nanoparticles of the composition $A^{II}B^{VI}$, the so-called "quantum dots," have intensively been studied for more than 20 years (see, e.g., Ref. 1). Many methods for their generation were proposed. The first syntheses were carried out predominantly in reversed micellar systems (see review²), whereas more recently high-temperature (up to 200 °C) reactions in homogeneous organic solutions using organometallic and organoelemental precursors became prevailing.^{3,4} This was related, in particular, to technological requirements and the necessity to develop methods for the preparative space production of quantum dots, which is difficult to accomplish in micellar solution.

Impressive success was achieved in this direction; however, the methods developed suffer from a number of drawbacks. These are, particularly, extreme conditions of synthesis and a high cost of reagents. In addition, the synthesis yields nanoparticles covered with a protective hydrophobic shell, for example, from triphenylphosphine oxide or long-chain carboxylic acids, whereas hydrophilized particles are required for some applications.

Therefore, alternative methods for the synthesis of quantum dots using aqueous solvents are developed in recent years.^{5–7} They are based on the use of traditional exchange reactions in solutions in the presence of various modifiers, which are adsorbed on the surface of nanoparticles formed and thus prevent their growth and aggregation. In particular, we have earlier shown^{8,9} that the interaction of zinc and copper salts with sodium sulfide in the presence of cysteine and other amino acids affords stable sols of nanoparticles of the corresponding sulfides with

the size about units of nanometers and a fairly narrow particle-size distribution. Nanoparticles of ZnS ~2 nm in size stabilized by glycine, methionine, or aspartic acid have intense luminescence and exhibit the properties of quantum dots.

The study of the "blank" process in the absence of a stabilizing modifier is needed to understand the mechanism of formation of these particles and the nature of their luminescence. At first sight, the problem seems strange, because the formation of the ZnS precipitate, which occurs upon pouring together the corresponding salts, is known since school-days and the ZnS sols have been studied in detail by specialists in colloid chemistry. However, the trends of modern science prompt researcher to return to the processes known long ago to carry out new studies using new equipment and investigation methods and in this way approach new challenges.

This work is aimed at studying the formation of zinc sulfide sols and precipitates by the exchange reaction in an aqueous solutions and the optical properties of ZnS particles that formed.

Experimental

Reagents $ZnSO_4 \cdot 7H_2O$ (Khimmed, pure grade) and $Na_2S \cdot 9H_2O$ (Sigma-Aldrich, 99%) were used. Distilled water was used for the preparation of working solutions in all experiments.

The images of zinc sulfide samples from precipitates were obtained on a LEO912 AB OMEGA transmission electron microscope (accelerating voltage 60, 80, 100, and 120 kV; illumination

area 1–75 μm ; illumination aperture 0.02–5 mrad; magnification 80–500 000 times; image resolution 0.2–0.34 nm; inelastic scattering energy resolution 1.5 eV; measurement region of inelastic scattering energy 0–2500 eV).

The X-ray phase analysis of precipitates was carried out with a Stoe Stad P powder diffractometer in the θ/θ geometry using $\text{CuK}\alpha$ radiation. The samples were scanned over the $15^\circ \leq 2\theta \leq 70^\circ$ range with an increment of 0.05° and a exposure to the dot of 10 s. The approximation method based on an analysis of the integral width of diffraction maxima was used to determine the mean size (d) of the coherent scattering region (CSR). The diffraction maximum (111) with an increment of 0.05° and a time of 50 s per dot was used to estimate the CSR of sphalerite.

The absorption spectra of zinc sulfide sols in water were recorded in quartz cells with an optical layer thickness of 10 mm on a Shimadzu UV-1800 spectrophotometer in the wavelength range 200–400 nm.

The luminescence spectra of zinc sulfide sols were measured in quartz cells with an optical layer thickness of 10 mm on a Fluorat-02-Panorama spectrofluorimeter (OOO Lyumeks). The luminescence excitation wavelength was chosen from the obtained absorption spectra.

Preparation of sols. Zinc sulfide as aqueous sols was obtained from the stock 0.5 *M* aqueous solutions of zinc sulfate and Na_2S by the double drop method at room temperature. For this purpose, equal volumes of the initial reactants were simultaneously added dropwise to a flask containing the necessary amount of distilled water from two burettes with permanent magnetic stirring of the reaction mixture. The average flow rate of reactant supply was 4 drop min^{-1} . In the case of formation of ZnS sols under the conditions of an excess (fivefold) of zinc ions (sulfur), 5 drops of a 0.5 *M* solution of ZnSO_4 (Na_2S) and then a drop of a 0.5 *M* solution of Na_2S (ZnSO_4) were added to water. The volume of water in the flask was calculated from the volumes of the drops in the burettes in such a way that the dilution of each drop to the 10^{-2} – 10^{-4} molar reaction concentration was attained. Zinc sulfide sols were prepared at room temperature in air, argon, or oxygen.

Preparation of precipitates. To prepare ZnS precipitates, 3 mL of the starting reactants were added using the double drop method to the necessary volume of water pre-heated to 25, 50, or 80 $^\circ\text{C}$. The obtained precipitates were centrifuged, washed with water 3–5 times, and dried in air to a constant weight.

Results and Discussion

The double drop method was used for the unification of the conditions for the synthesis of both sols and precipitates.^{9,10} The method is based on the slow simultaneous addition of concentrated (0.5 *M*) solutions of zinc sulfate and sodium sulfide to a large volume of an aqueous solution. By adding each portion of the reactants the solution is diluted 2–4 orders of magnitude, and this dilution remains almost unchanged during the whole synthesis. In addition, each new portion of zinc sulfide is formed under the same conditions in the absence of "extra" Zn^{2+} and S^{2-} ions capable of specific adsorption on the surface of the formed particles.

The ZnS precipitates obtained at various reaction concentrations of the reactants were studied by transmission electron microscopy (TEM) and X-ray diffraction analysis. One of the most characteristic TEM images is presented in Fig. 1. It is seen that the zinc sulfide precipitate consists of aggregates of varying sizes and shapes, and the aggregates, in turn, consist of finer and more uniform in shape and size "primary" particles. The mean size of these particles depends on the reaction concentration of the reactants, increasing from 2.4 to 3.8 nm with an increase in the concentration $[\text{Zn}^{2+}] = [\text{S}^{2-}]$ from 10^{-4} to 10^{-3} mol L^{-1} . The data spread is ± 0.5 and ± 0.7 nm, respectively, although this estimate is rather conventional for the system studied because of the irregular particle shape and difficulties encountered in the analysis of the images.

According to the X-ray diffraction data, the obtained zinc sulfide precipitates are characterized by the crystal structure corresponding to the cubic modification of ZnS (sphalerite). The mean size of the coherent scattering region (CSR) of the primary ZnS particles estimated from the Debye–Scherrer formula¹¹ is 2.4 nm for the reaction concentrations $[\text{Zn}^{2+}] = [\text{S}^{2-}] = 1 \cdot 10^{-3}$ mol L^{-1} . This agrees satisfactorily with the TEM data that are, as a rule, in excess of the results calculated from X-ray diffraction analysis.

In addition to the concentration of the reactants, the synthesis temperature can affect the size of the formed particles. In this work, we showed that the mean CSR size of the primary particles in the ZnS precipitates obtained at 25, 50, and 80 $^\circ\text{C}$ and the reaction concentration $[\text{Zn}^{2+}] = [\text{S}^{2-}] = 1 \cdot 10^{-3}$ mol L^{-1} increases with the temperature of the synthesis, being 2.4 ± 0.1 , 2.8 ± 0.1 , and 3.2 ± 0.2 nm, respectively.

To reveal the mechanism of formation of zinc sulfide nanoparticles, we applied absorption spectrometry to study

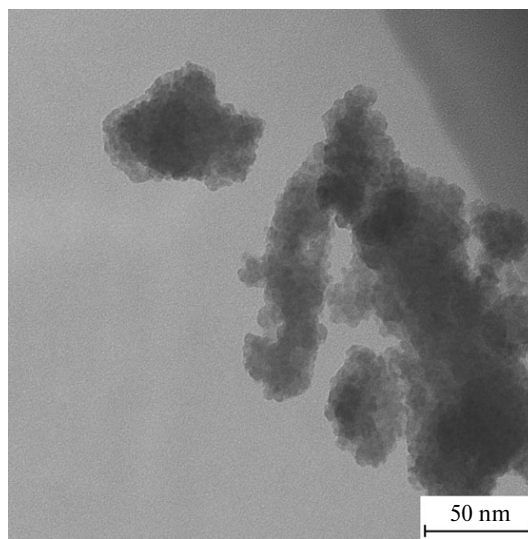


Fig. 1. TEM images of the ZnS precipitate prepared by the double drop method.

the ZnS sols formed. It is known¹² that for semiconductor nanoparticles, including ZnS, the ratio between the optical absorption coefficient α and the energy $h\nu$ absorbed during irradiation is described as follows:

$$(\alpha h\nu) = A (h\nu - E_i)^n, \quad (1)$$

where A is coefficient, E_i is the forbidden band of the semiconductor nanoparticle, and the value of n depends on the type of electron transition from the valence band to the conductance band in the semiconductor upon excitation. For ZnS, $n = 1/2$ was used.¹³ This makes it possible to estimate the value of the forbidden band E_i of nanoparticles in the sols, which is related to the particle size $d = 2r$ as follows^{12–14}:

$$\Delta E = E_i - E_g = \hbar^2 \pi^2 / 2\mu r_i^2, \quad (2)$$

where ΔE is the difference between the forbidden band gap of a nanoparticle (E_i) and the forbidden band gap of a bulky crystal (E_g) (in the case of ZnS, $E_g = 3.65$ eV), \hbar is the reduced Planck's constant ($\hbar = (h/2\pi)$, eV s), μ is the reduced mass of an exciton (for ZnS, $\mu = 0.176 m_e$),¹⁴ m_e is the mass of an electron equal to $9.1 \cdot 10^{-31}$ kg, and r_i is the radius of a nanoparticle under the assumption of its spherical shape.

The typical UV absorption spectrum of the zinc sulfide sol, its transformation into the dependence $\alpha^2 E^2 = f(E)$, and the determination of E_i from the inclined region of the absorption edge of the obtained curve are shown in Fig. 2. The spectra of all sols obtained in this work were processed similarly. The insertion of the corresponding values of E_i into Eq. (2) made it possible to estimate the sizes of the primary ZnS particles in the sol.

Some of the obtained results are given in Table 1. The method of absorption spectroscopy confirmed the above

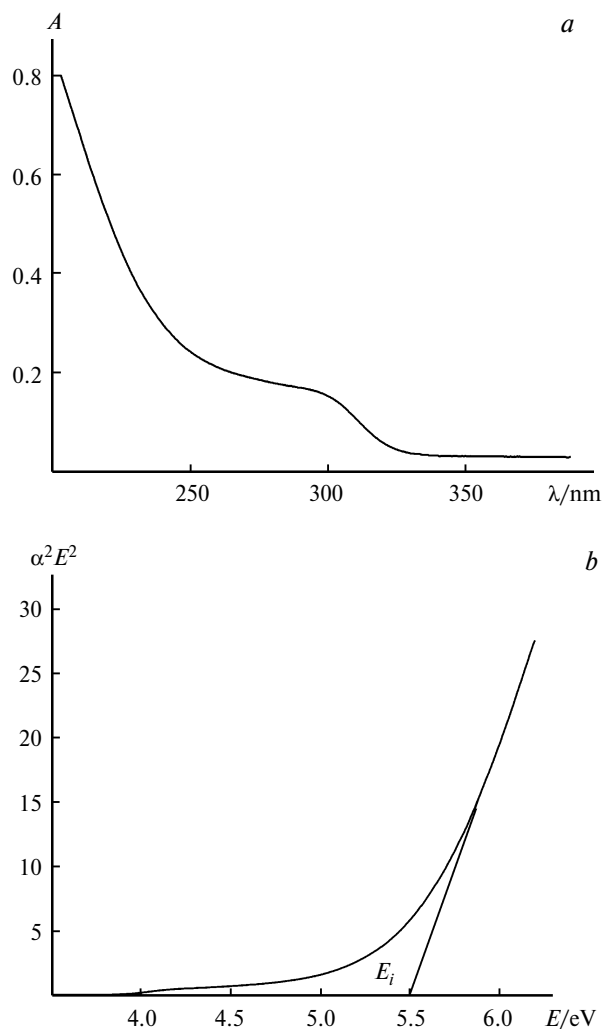


Fig. 2. UV spectrum of the ZnS sol at $[Zn^{2+}] = [S^{2-}] = 1 \cdot 10^{-4}$ mol L⁻¹ in the coordinates $A(\lambda)$ (a) and $f(E) = \alpha^2 E^2$ (b).

Table 1. Mean size of primary particles in the ZnS sols under different concentration conditions of sol preparation

Entry	Conditions of sol preparation*		Reaction concentration		d/nm
	$V_{ZnSO_4} = V_{Na_2S}$	V_{H_2O}	$[Zn^{2+}] = [S^{2-}]$	$[ZnS]$	
	ml		mol L ⁻¹		
1	0.04	200	$1 \cdot 10^{-4}$	$1 \cdot 10^{-4}$	2.1
2	0.20	200	$1 \cdot 10^{-4}$	$5 \cdot 10^{-4}$	2.4
3	0.40	200	$1 \cdot 10^{-4}$	$1 \cdot 10^{-3}$	2.6
4	0.04	40	$5 \cdot 10^{-4}$	$5 \cdot 10^{-4}$	2.3
5	0.04	20	$1 \cdot 10^{-3}$	$1 \cdot 10^{-3}$	2.5
6**	0.04	6	$3.3 \cdot 10^{-3}$	$3.3 \cdot 10^{-3}$	2.6
7**	0.04	2	$1 \cdot 10^{-2}$	$1 \cdot 10^{-2}$	3.1

* $[Zn^{2+}] = [S^{2-}] = 0.5$ mol L⁻¹

** Immediately after formation, the sols were diluted with water to the concentration $[ZnS] = 10^{-4}$ mol L⁻¹.

notion that the zinc sulfide primary particles tend to grow with an increase in the reaction concentrations of the precursors (entries 1, 4–7). This is also accompanied by the growth of the particles during the accumulation of the final reaction product at unchanged reaction concentrations of ZnSO₄ and Na₂S (entries 1–3). Thus, two processes occur in the solution: the formation of new particles and the precipitation of already existing particles on the surface. The estimations show that the former process prevails. It should be expected that the mean sizes of the primary zinc sulfide particles in the precipitates should be larger than those in the sols.

Since the practical use of zinc sulfide is mainly related to its optical properties, at the next stage of the work we studied the luminescence properties of the ZnS sols obtained by the synthesis method used. For this purpose, the starting reactants were added to the necessary volume of water with permanent stirring at room temperature in air,

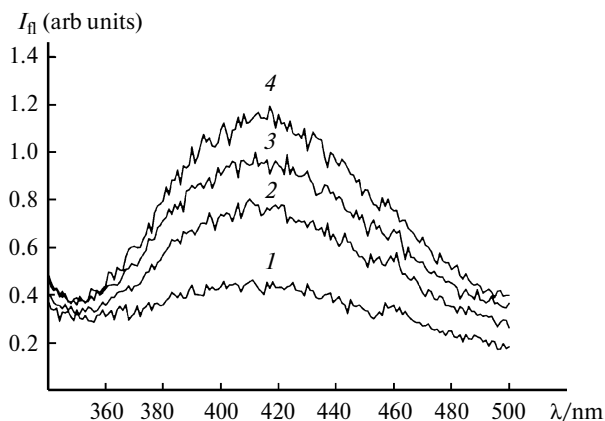


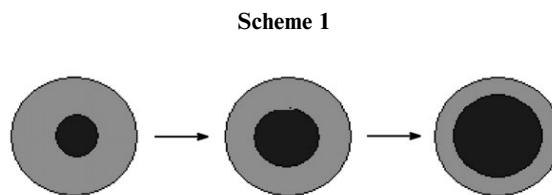
Fig. 3. Change in the fluorescence intensity of the ZnS at intervals of 1 (1), 3 (2), 7 (3), and 11 min (4); $[\text{Zn}^{2+}] = [\text{S}^{2-}] = 1 \cdot 10^{-3} \text{ mol L}^{-1}$.

after which an aliquot with the sol was rapidly transferred to the cell of the luminometer. As can be seen from Fig. 3, the zinc sulfide sol has the fluorescence properties, and its emission spectra are presented by a broad band with the radiation intensity maximum at $\lambda_f \approx 425 \text{ nm}$.

It is known^{11,15} that fluorescence of zinc sulfide (which was not specially alloyed) is caused by intrinsic defects of its crystalline lattice, such as vacancies of zinc and sulfur atoms (V_{Zn} and V_{S}) and interstitial zinc and sulfur atoms (I_{Zn} and I_{S}). The fluorescence intensity maxima at $\lambda = 416$ and 424 nm correspond to the optical transitions from the levels of the interstitial sulfur and zinc atoms, respectively (see Ref. 16), and those at $\lambda = 430$ and 438 nm correspond to the optical transitions from the levels of sulfur and zinc vacancies, respectively. A comparison of these data with our results clarifies the large width of the fluorescence band, which is a superposition of isolated closely lying bands corresponding to the described optical transitions.

It is seen from Fig. 3 that the fluorescence intensity of the sol increases ~ 3 times within the first ~ 10 min. Then the fluorescence intensity decreases slowly with aggregation and coagulation (this groups of spectra is omitted). The relationship between the fluorescence and defects of the crystalline lattice of zinc sulfide assumes that the increase in the signal intensity with time is due to the accumulation of defects in the zinc sulfide particles. It is possible that, at the first moment, particles with a considerable fraction of the amorphous phase are formed as a shell on the core of the crystal nucleus, and then the particle "ripens" via the mechanism of the so-called intragrain recrystallization of the substance.¹¹ The growth of the crystalline core within each primary particle can be presented by Scheme 1.

According to Scheme 1, the internal part of the primary particle increases with time and the thickness of the non-equilibrium disordered external layer decreases whereas overall diameter of the particle remains relatively constant. It is most likely that these fine processes are reflect-



ed in the dynamics of the signal intensity in the fluorescence spectra.

To elucidate the influence of intrinsic defects on the optical properties of aqueous sols of zinc sulfide, we carried out an additional series of experiments. In these experiments, sol formation was investigated under the conditions that involved either a fivefold excess or deficiency of zinc or sulfur ions at the equal concentration of zinc sulfide in the reaction medium. Since the position of the intensity maximum of the signal in the absorption spectra of the ZnS sols formed in zinc ion excess (Fig. 4, curve 2) is observed at $\lambda \approx 280 \text{ nm}$, whereas in sulfur ion excess it lies at $\lambda \approx 290 \text{ nm}$ (Fig. 4, curve 3), the corresponding fluorescence spectra were recorded at an interval of 3 min at the both excitation wavelengths (Fig. 5).

The maxima are detected at the fundamental absorption edge, indicating the presence of energy levels inside the forbidden crystal band caused by defects of different nature. As can be seen from the fluorescence spectra (see Fig. 5), the maximum intensity of the signal and the highest value of its maximum are observed for the ZnS sol formed with Zn^{2+} excess and detected at the optimum excitation wavelength $\lambda_{\text{exc}} = 280 \text{ nm}$. With S^{2-} excess, the maximum fluorescence intensity ($\lambda_{\text{exc}} = 290 \text{ nm}$) decreases threefold, and at the equimolar ratio of Zn^{2+} to S^{2-} this value occupies some intermediate position. All these data suggest that the luminescence of the obtained sols is due predominantly to the defect character of the ZnS crystal structure related to the zinc ions.

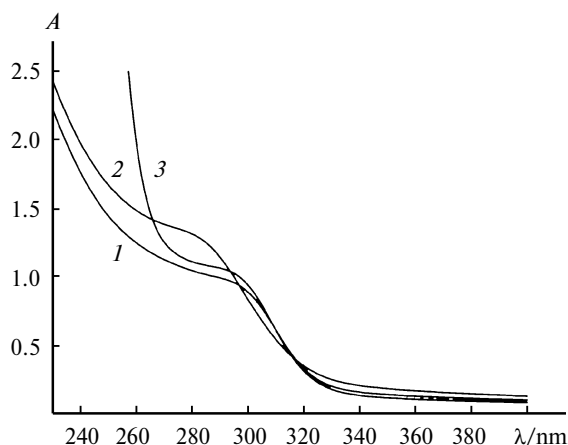


Fig. 4. UV spectra of the ZnS sols formed at $\text{Zn} : \text{S} = 1 : 1$ (1), $5 : 1$ (2), and $1 : 5$ (3); $[\text{ZnS}] = 5 \cdot 10^{-4} \text{ mol L}^{-1}$.

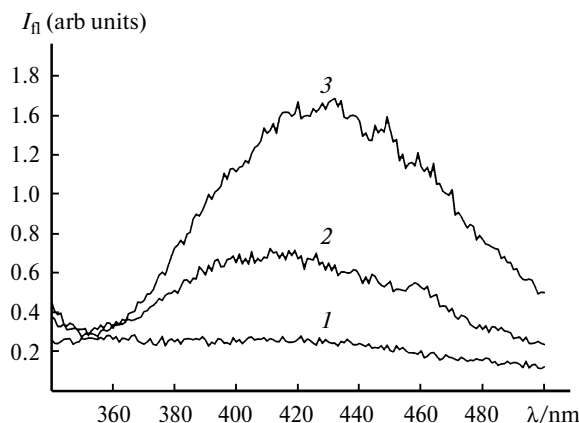


Fig. 5. Fluorescence spectra of the ZnS sols formed at Zn : S = 1 : 5 (1), 1 : 1 (2), and 5 : 1 (3); $[\text{ZnS}] = 5 \cdot 10^{-4} \text{ mol L}^{-1}$.

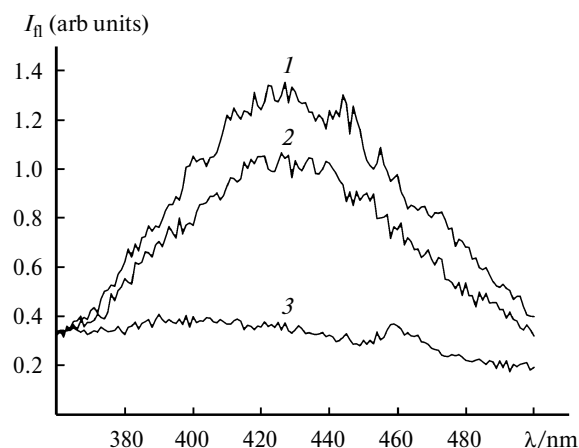


Fig. 6. Fluorescence spectra of the ZnS sols obtained in water saturated with air (1) or oxygen (2) and distilled under argon (3); Zn : S = 1 : 1, $[\text{ZnS}] = 1 \cdot 10^{-3} \text{ mol L}^{-1}$, $\lambda_{\text{exc}} = 290 \text{ nm}$.

In addition to intrinsic defects, oxygen also plays an important role in generating the optical properties of zinc sulfide,¹⁷ because it is an isoelectronic admixture introducing defects to the semiconductor structure. To reveal this problem, the sols were synthesized in water distilled in air or in argon. A number of syntheses were accomplished in water stored in oxygen under 5 atm for 24 h. All sols were formed under the conditions of Zn/S = 1/1 at room temperature. Figure 6 shows that in an anaerobic medium the fluorescence intensity of the ZnS sols is sharply decreased compared to that in aerobic media.

This study showed that the zinc sulfide precipitates obtained by the double drop method are aggregates of nanoparticles about 3 nm in size. The mean particle size increases with an increase in the concentration of the re-

actants and temperature, but this effect is insignificant (a 1.5-fold increase). At the first step, particles with a considerable fraction of the amorphous phase are formed and undergo intragrain crystallization within at least 10 min. The ZnS nanoparticles that formed have the luminescence properties predominantly caused by the defect character of the crystalline lattice related to zinc ions and to oxygen admixtures.

This work was financially supported by the Russian Foundation for Basic Research (Project No. 09-03-00875a).

References

1. A. Henglein, *Chem. Rev.*, 1989, **89**, 1861.
2. B. D. Summ, N. I. Ivanova, *Usp. Khim.*, 2000, **69**, 995 [*Russ. Chem. Rev. (Engl. Transl.)*, 2000, **69**].
3. X. Li, S. Sun, H. Yu, W. Zhang, W. Fan, Y. Yang, *J. Mater. Sci.*, 2004, **39**, 659.
4. C. B. Murray, D. J. Norris, M. G. Bawendi, *J. Am. Chem. Soc.*, 1993, **115**, 8706.
5. I. Umezu, R. Koizumi, K. Mandai, T. Aoki-Matsumoto, K. Mizuno, M. Inada, A. Sugimura, Y. Sunaga, T. Ishii, Y. Nagasaki, *Microelectronic Engineering*, 2003, **66**, 53.
6. H. Li, W. Y. Shih, W.-H. Shih, *Nanotechnology*, **18**, 205604.
7. Z. Li, J. Wang, X. Xu, X. Ye, *Mater. Letters*, 2008, **62**, 3862.
8. H. V. Ehrlich, T. N. Shcherba, M. P. Zhilenko, G. P. Muravieva, G. V. Lisichkin, *Zh. Obshch. Khim.*, 2010, 939 [*Russ. J. Gen. Chem. (Engl. Transl.)*, 2010, **80**, 1109].
9. M. P. Zhilenko, K. V. Lupandina, H. V. Ehrlich, G. V. Lisichkin, *Izv. Akad. Nauk, Ser. Khim.*, 2010, 1277 [*Russ. Chem. Bull., Int. Ed.*, 2010, **59**, 1307].
10. M. P. Zhilenko, H. V. Ehrlich, G. V. Lisichkin, *Rossiiskie nanotekhnologii* [*Russ. Nanotechnol.*], 2009, **4**, 64.
11. A. M. Gurvich, *Vvedenie v fizicheskuyu khimiyu kristallofobov* [*The Introduction into the Physical Chemistry of Crystallophores*], Vysshaya Shkola, Moscow, 1982, 376 pp. (in Russian).
12. R. F. Khairutdinov, *Kolloid. Zh. [Colloidal Journal]*, 1997, **59**, 581 (in Russian).
13. S. Kuldeep, D. Rathore, Y. Patidar, Y. Janu, N. S. Saxena, Kananbala Sharma, T. P. Sharma, *Chalcogenide Letters*, 2008, **5**, 105.
14. S. Wageh, L. Shu-Man, F. T. You, X. Xu-Rong, *J. Luminescence*, 2003, **102–103**, 768.
15. D. Curie, *Luminescence cristalline*, Dunod, Paris, 1960.
16. D. Denzler, M. Olschewski, K. Sattler, *J. Appl. Phys.*, 1998, **84**, 2841.
17. N. K. Morozova, V. A. Kuznetsov, *Sul'fid tsinka. Poluchenie i opticheskie svoistva* [*Zinc Sulfide. Synthesis and Optical Properties*], Moscow, 1987, 200 pp. (in Russian).

Received October 20, 2010;
in revised form January 17, 2011